Thermophysical Properties of Interfacial Layer in Nanofluids

Donggeun Lee*

School of Mechanical Engineering, RIMT, Pusan National University, 30 Jangjeon-dong, Geumjeong-gu, Busan 609-735, Korea

Received October 21, 2006. In Final Form: December 18, 2006

Although recent experiments have revealed that nanofluids have superior thermal conductivities to base fluids, the inherent physics are not fully understood. In this study, an interfacial layer, competing with Brownian motion as a corresponding mechanism, is conceptually connected with the surface-charge-induced electrical double layer. By applying colloidal science, the first explicit equations for the thickness and thermal conductivity of the layer are obtained. A fractal model including the new concept of the layer is developed. The model predictions are compared with experimental data for effects of pH, temperature, volume fraction, and primary particle size of CuO−water nanofluids.

1. Introduction

Nanofluid, a colloidal liquid with nanoparticles, has increasingly attracted worldwide attention, since 1995 when Choi[1] introduced a new kind of the heat-transport fluid. Many experimental results have followed the unbelievable report[2] of Choi and his colleagues in 2001, citing more than 150% increase in effective thermal conductivity K_{eff} of carbon nanotube−olefin oil nanofluid with respect to that of the base fluid K_f. The mainstream experimental research was to find the best combination of particles and solvents[3−17] and to find the most significant systematic parameters as well. The parameters may be sorted into three classes, i.e., particle-related, fluid-related, and interrelated parameters. The first kind includes size,[3−5] morphology (elongated,[2,6] spherical,[3,7,8] and mass fractal-like[9−14] shapes), and volume fraction of particles. The second would be thermophysical properties of the base fluid such as viscosity, thermal conductivity, and temperature.[3,10,15] Interface chemical effect or interaction between the particles and base fluid[6,14] would correspond to the last class.

Besides great interest in the K_{eff} of the nanofluid, several groups initiated investigation of more practical application fields such as microchannel heat sink,[18] forced convective heat transfer fluids,[19] and a lubricating fluid with high thermal conductivity.[20] Although nanofluids in the field certainly look promising, it is not rare to find large discrepancies among the experimental data obtained by different research groups. Keblinski et al.[21] addressed this as one of the primary obstacles to the development of nanofluids. Also, they concluded that poor characterization of the suspension, e.g., quantifying how stable the colloid is, could explain the inconsistencies in experiments in terms of inconsistent initial conditions of the nanofluids. Recently, we demonstrated that pH of the CuO−water nanofluid controlled the surface charge states as well as the interaction potentials. By using the Derjaguin−Landau−Verwey−Overbeek (DLVO) linearized mean field theory,[22] we successfully quantified the suspension stability of the nanofluid and found that the K_{eff} was strongly correlated with the surface charge states.[14] Right after this study, Prasher et al.[23] suggested that the K_{eff} could be greatly changed by aggregation kinetics and the characteristic time for aggregation was influenced by various systematic parameters. Therefore, it is necessary to know a complete set of the three classes of parameters for a model evaluation or even for a fair comparison between experiments.

Keblinski et al.[24] who gave the first reasonable insights of the mechanisms showed that Brownian motion (BM) was not responsible for the enhancement of the K_{eff}. However, a few groups such as Jang and Choi,[25] Kumar et al.,[26] and Prasher et al.[27] are still arguing that the motion-related effect plays a dominant role, though their predictions were made with

* Author to whom correspondence should be addressed. Electronic mail: donglee@pusan.ac.kr. Tel +82-51-510-2365. Fax +82-51-512-5236.

(1) Choi, S. U. S. *ASME FED* **1995**, *231*, 99.
(2) Choi, S. U. S.; Zhang, Z. G.; Yu, W.; Lockwood, F. E.; Grulke, E. A. *Appl. Phys. Lett.* **2001**, *79*, 2252.
(3) Patel, H. E.; Das, S. K.; Sundararajan, T.; Nair, A. S.; George, B.; Pradeep, T. *Appl. Phys. Lett.* **2003**, *83*, 2931−2934.
(4) Xie, H.; Wang, J.; Xi, T.; Liu, Y.; Ai, F.; Wu, Q. *J. Appl. Phys.* **2002**, *91*, 4568−4572.
(5) Chon, C. H.; Kihm, K. D.; Lee, S. P.; Choi, S. U. S. *Appl. Phys. Lett.* **2005**, *87*, 153107.
(6) Xie, H.; Lee, H.; Youn, W.; Choi, M. *J. Appl. Phys.* **2003**, *94*, 4967−4971.
(7) Eastman, J. A.; Choi, S. U. S.; Li, S.; Yu, W.; Thompson, L. J. *Appl. Phys. Lett.* **2001**, *78*, 718−720.
(8) Xie, H.; Wang, J.; Xi, T.; Liu, Y. *Int. J. Thermophys.* **2002**, *23*, 571−580.
(9) Xuan, Y.; Li, Q. *Int. J. Heat Fluid Flow* **2000**, *21*, 58−64.
(10) Das, S. K.; Putra, N.; Thiesen, P.; Roetzel, W. *J. Heat Transfer* **2003**, *125*, 567−574.
(11) Lee, S.; Choi, S. U. S.; Li, S.; Eastman, J. A. *J. Heat Transfer* **1999**, *121*, 280−288.
(12) Murshed, S. M. S.; Leong, K. C.; Yang, C. *Int. J. Therm. Sci.* **2005**, *44*, 367−373.
(13) Xuan, Y.; Li, Q.; Hu, W. *AIChE J.* **2003**, *49*, 1038−1043.
(14) Lee, D.; Kim, J.-W.; Kim, B. G. *J. Phys. Chem. B* **2006**, *110*, 4323−4328.
(15) Li, C. H.; Peterson, G. P. *J. Appl. Phys.* **2006**, *99*, 084314.
(16) Eastman, J. A.; Choi, S. U. S.; Li, S.; Thompson, L. J.; Lee, S. In *Nanophase and Nanocomposite Materials II*; Komarneni, S., Parker, J. C., Wollenberger, H. J., Eds.; *Material Research Society Symposium Proceedings*: Pittsburgh, 1997; pp 3−11.
(17) Wang, B.-X.; Zhou, L.-P.; Peng, X.-F. *Int. J. Heat Mass Transfer* **2003**, *46*, 2665−2672.
(18) Jang, S. P.; Choi, S. U. S. *Appl. Therm. Eng.* **2006**, *26*, 2457−2463.
(19) Heris, S. Z.; Etemad, S. G.; Esfahany, M. N. *Int. Commun. Heat Mass Transfer* **2006**, *33*, 529−535.
(20) Hwang, Y.; Park, H. S.; Lee, J. K.; Jung, W. H. *Curr. Appl. Phys.* 2006, in press.
(21) Keblinski, P.; Eastman, J. A.; Cahill, D. G. In *Materials Today*; Elsevier; June, 2005; pp 36−44.
(22) Hunter, R. J. *Foundations of Colloid Science*, 1st ed.; Clarendon Press: Oxford, 1987.
(23) Prasher, R.; Phelan, P. E.; Bhattacharya, P. *Nano Lett.* **2006**, *6*, 1529−1534.
(24) Keblinski, P.; Phillpot, S. R.; Choi, S. U. S.; Eastman, J. A. *Int. J. Heat Mass Transfer* **2002**, *45*, 855−863.
(25) Jang, S. P.; Choi, S. U. S. *Appl. Phys. Lett.* **2004**, *84*, 4316−4318.
(26) Kumar, D. H.; Patel, H. E.; Kumar, V. R. R.; Sundararajan, T.; Pradeep, T.; Das, S. K. *Phys. Rev. Lett.* **2004**, *93*, 144301.
(27) Prasher, R.; Bhattacharya, P.; Phelan, P. E. *Phys. Rev. Lett.* **2005**, *94*, 025901.

10.1021/la063094k CCC: $37.00
Published on Web 04/19/2007

different equations. It is notable that the groups have all disregarded that the metal oxide particles used for the model evaluation were highly aggregated (see ref 16 in Jang and Choi,[25] ref 14 in Kumar et al., [26] and refs 1 and 4 in Prasher et al.[27]). Since aggregation of isolated (primary) particles decreases the speed at which particles are moving, use of the primary particle size can considerably overestimate the effect of the BM. Recent molecular dynamic simulation[28] reveals that the hydrodynamic BM mechanism has only a minor effect on the K_{eff} even for a relatively high dose of nanoparticles (ca. 3.3 vol %). In this regard, the BM effect is not taken into account in this study.

On the other hand, some people have proposed a hypothetical concept of the ordered liquid layering around the particle−liquid interface as another reason for the enhancement of the K_{eff}.[17,24,29−31] The good predictions with relevant models were, however, based on arbitrarily assumed values for thickness and thermal conductivity of the interfacial layer. Under the assumption of constant properties of the layer, any versions of the relevant model have never explained the pH dependence of the K_{eff}[14] or the influence of the surface modification.[3,6] The last mechanism suggested by Keblinski et al.[24] is a percolation behavior of heat transport especially when the colloidal particles are agglomerated. The heat is preferably transferred through the aggregate backbone in a liquid sphere,[23] so that the nanofluid containing aggregates may have higher effective thermal conductivity, compared to the case of disassembling the aggregates into their primary particles.

In this study, the author attempts to connect the concept of an interfacial layer with an electrical double layer (EDL) forming around the surfaces of particles in suspension. The thickness and thermal conductivity of the interfacial layer thereby have functional dependencies on systematic parameters. Regarding this, the author proposes a mathematical fractal model incorporating the afore-mentioned parameters and mechanisms. Quantitative comparisons of the model with the various experimental data will be seen.

2. Experimental Section

The experimental procedures from the sample preparation to the characterization of the colloid[14] are revisited in view of a full set of data and briefly addressed as follows. As-received CuO nanoparticles (Aldrich, cat. no 54486−8) are highly agglomerated. Right after the particles are immersed into deionized water, the colloid is strongly agitated with 700 W ultrasonic waves. Such a high-powered ultrasonic treatment is thought in general to improve the stability of the colloids by tearing the agglomerates into their primary particles. But, many tests for different durations and powers of ultrasonication (Jeiotech, Kr., ULH-700S) revealed that the particles sustain their fractal shapes (see Figure 1 in ref 14).

A photon correlation method (Otsuka Electronics, Jp., ELS-8000) was used to estimate hydrodynamic radius R_h of particles moving in liquid[14,22] through the measurement of diffusion coefficient of the particles. As far as Brownian motion of aggregates concerns, the R_h of aggregates is more important than the radius of their primary particles a. It is surprising that most of researchers claiming the BM mechanism have not attempted to measure the R_h. Figure 1shows that the R_h of CuO aggregates in water ranges from 90 nm to 140 nm, depending on the pH of the nanofluid, whereas a was estimated to about 17.5 nm. Such large aggregates seem to be too big to generate any apparent size effect.[25]

The pH of the colloids was altered by adding suitable amounts of HCl or NaOH (Aldrich, cat. no 31894−9 or 30657−6, respectively). NaCl (Aldrich, cat. no 20443−9) as an electrolyte was used for keeping the total ionic strength consistent, but the dose

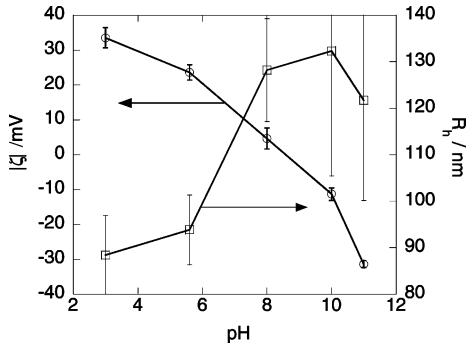

Figure 1. Effect of the pH of a CuO−water nanofluid on the suspension stability: the measurements are made at $T = 25$ °C and $\phi_{exp} = 0.003$. The error bars represent standard deviations of data from more than 10 measurements.

level was much lower than the critical value (ca. 5×10^{-2} mol dm^{-3}) at which particles are settled by a violent aggregation. The volume fraction of particles is kept constant at 0.3% during the experiments. Effective thermal conductivity (K_{eff}) of the fluid is measured at 25 °C by a conventional transient hot wire device. The zeta potential ζ of the nanofluid measured from electrokinetic data (Otsuka Electronics, Jp., ELS-8000) was combined with a surface complexation model to obtain surface charge states. More details of the experimental and theoretical procedures are explained elsewhere.[14] The author notes that these data are pretty close to the complete data set which was mentioned in the Introduction. The whole sets of the data at different pHs will be basically used for evaluating the present model. As such data have not been reported for other materials, further evaluation of the model will be limited to the CuO−water nanofluid in the literature. The model predictions for the influences of volume fraction, temperature, and primary particle size will also be presented.

3. Thermophysical Properties of Surface Charge-Induced Interfacial Layer

A. Thickness of Interfacial Layer (*t*). When materials such as oxides, sulfides, and insoluble salts are immersed in aqueous solution, they acquire surface charges, the presence of which builds up the surface electrostatic potentials. The surface charges attract and bind counterions with opposite polarity in liquid. Regarding that the ions are often hydrated, one may postulate that association of such ions with water molecules at the interface is the origin of the hypothetical charge-induced interfacial layer in the literature. The alternating alignment of the (often hydrated) ions may form liquid columns as depicted in Figure 2 with a bold-dotted box. The strong ionic bonds between the surface and the columns seem likely to reduce the Kapitza resistance significantly and make arrangements of the ions mimic the crystal structure of solid atoms at the surface as well. More detail mechanism about the EDL is described elsewhere.[14,22]

Since the thickness of the EDL often scales as a reciprocal Debye−Huckel parameter κ^{-1} $(=\sqrt{\epsilon_0\epsilon_r R_0 T/2000F^2 I})$,[14,22] the thickness t can be expressed as

$$t = C\kappa^{-1} \tag{1}$$

where ϵ_0 is vacuum permittivity, F is Faraday constant, and R_0 is gas constant. The remaining properties such as dielectric constant ϵ_r, ionic strength I, and temperature T are all related to the solution. Thus, the thickness of the interfacial layer has now base-fluid dependence. In particular, increasing the temperature makes the layer thicker, resulting in an increase of the apparent volume fraction, through which the K_{eff} of nanofluids can then

(28) Evans, W.; Fish, J.; Keblinski, P. *Appl. Phys. Lett.* **2006**, *88*, 093116.
(29) Xue, Q.; Xu, W.-M. *Mater. Chem. Phys.* **2005**, *90*, 298−301.
(30) Yu, W.; Choi, S. U. S. *J. Nanopart. Res.* **2003**, *5*, 167−171.
(31) Xue, Q. Z. *Phys. Lett. A* **2003**, *307*, 313−317.

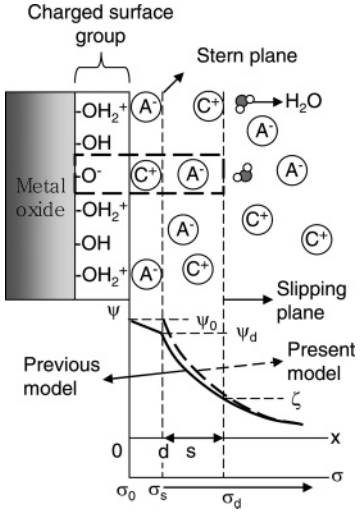

Figure 2. Structure of electrical double layer (EDL) formed at the metal oxide−water interface:[14,22] dehydrated counterion A^- or C^+ bonded strongly to the charged group at surface forms an immobile part of the EDL (stern layer). In contrast, in the outer region named as a diffuse layer, such ions are bound weakly, resulting in gradual decrease in the potential. The σ_0, σ_s, and σ_d are charge densities at the surface (0 plane), in the stern plane, and in the diffuse layer, respectively.

be enhanced. The temperature dependence which has been thought to be a justification of the BM models[25−27] can also be explained by the concept of the interfacial layer.[17,24,29−31]

In the present condition, pH of solution can alter the κ^{-1} through the ionic strength *I*. For example, when the pH increases from 3 to 8, keeping the other parameters constant, the κ^{-1} increases from 7 to 13 nm. Taking κ^{-1} as the layer thickness *t* ($C = 1$), the *t* value is comparable to the primary particle radius of 17.5 nm but negligible compared to the R_h (from 90 to 140 nm) of the aggregates. As the primary particles get smaller, the contribution of the layer become greater.

B. Thermal Conductivity of Interfacial Layer (K_l). When recounting the concept of "liquid column" described in the previous section, if there exist more sites to launch the column (total charged surface density Γ_{ion}) and more ions to strengthen the column structure (ion density in the EDL given by $\sigma_d\kappa$, i.e., the product of charge density in the diffusive plane σ_d and the Debye−Huckel parameter κ),[14] this would in turn facilitate phonon transport from particle to liquid.[32] Interestingly, the experiment revealed that K_{eff} was expressed well as a power of $\Gamma_{ion}\sigma_d\kappa$.[14] Hence, it seems plausible to assume that the thermal conductivity of the layer K_l is also expressed as a power function of $\Gamma_{ion}\sigma_d\kappa$. Note that the K_l of the EDL is limited by two extremes, i.e., K_f and K_s (thermal conductivity of the CuO). The upper limit ($K_l = K_s$) would be the case at the condition for complete ionization of the surface ($\Gamma_{ion} = \Gamma_{tot} = 5.88 \times 10^{-6}$ mol m^{-2}) and maximizing $\sigma_d\kappa$ (at pH = 3). In this way, one may derive a reasonable functional relationship between K_l and $\Gamma_{ion}\sigma_d\kappa$ as

$$\frac{K_l - K_f}{K_s - K_f} = \left[\frac{(\Gamma_{ion}\sigma_d\kappa)_{pH}}{\Gamma_{tot}(\sigma_d\kappa)_{pH=3}}\right]^{\alpha} \quad (2)$$

The exponent α is an adjustable parameter for fitting the experimental data. However, once α has been determined, the value was a fixed constant throughout all predictions. In eq 2, the K_l value has an implicit temperature dependence through the terms of Γ_{ion}, σ_d, and κ. The validity of the equation will be discussed in the Discussion. In the Appendix, a theoretical procedure to estimate the surface charge states is described in detail, which is modified to consider varying temperatures on the basis of the previous theory.[14]

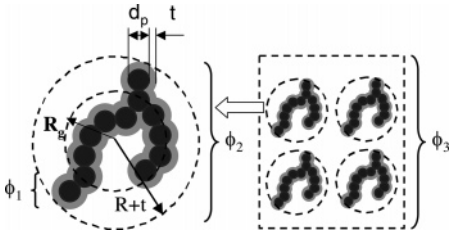

Figure 3. Geometrical configuration of fractal aggregates covered with interfacial layer in a nanofluid.

4. Fractal Model

The fractal feature of aggregates is generally described by the following power law.[33−35] The number of primary particles N_p within an aggregate scales as the outer radius *R* or the radius of gyration R_g with respect to the radius of primary particles *a*

$$N_p = k_0\left(\frac{R}{a}\right)^{D_f} = k_g\left(\frac{R_g}{a}\right)^{D_f} \quad (3)$$

where D_f is a fractal dimension, and k_0 and k_g are prefactors based on *R* and R_g, respectively. Koylu et al.[33] performed a computer simulation for a diffusion-limited cluster−cluster aggregation and concluded that k_0 is related to k_g as a function of D_f as

$$k_0 = k_g\left(\frac{D_f}{D_f + 2}\right)^{D_f/2} \quad (4)$$

The D_f value can be estimated from the slope of a log−log plot of N_p against R/a according to eq 3 and ranges typically from 1.5 to 1.8 for the present shape of aggregates.[13,17,33−35] Also, the k_0 obtained from the *y*-intercept in the plot is typically close to unity. The values of $D_f = 1.6$ and $k_0 = 1.34$ taken for the best fit in this study are comparable to those of Kim and Yuan,[35] $D_f = 1.67$ and $k_0 = 0.83$; Wang et al.,[17] $D_f = 1.57$ and $k_0 = 1.0$; Xuan et al.,[13] $D_f = 1.51$ and $k_0 = 1.07$; and Lee and Choi,[34] $D_f = 1.7$ and $k_0 = 1.34$. Substituting eq 4 to eq 3 gives

$$R_g = R\left(\frac{D_f}{D_f + 2}\right)^{1/2} \quad (5)$$

While drying the sampled nanofluid on a grid for TEM observation, aggregates are moved and sometimes overlapped on the grid, which often makes it difficult to measure *R* precisely, whereas light scattering can directly measure R_h,[14,22] which approximates R_g within 13% error.[35] *R* and N_p are then obtained with given values of R_g, D_f, and d_p by eqs 3 and 5, respectively. Those are delivered to the following model for prediction of K_{eff}.

Similarly to the treatment of an aggregate presented by Wang et al.,[17] the present model consists of three sequential steps, from a primary particle with the EDL to the whole system of nanofluid via an equivalent sphere including an aggregate. Figure 3 shows

(32) Xue, L.; Keblinski, P.; Phillpot, S. R.; Choi, S. U. S.; Eastman, J. A. *J. Chem. Phys.* **2003**, *118*, 337−339.
(33) Koylu, U. O.; Faeth, G. M.; Farias, T. L.; Carvalho, M. G. *Combust. Flame* **1995**, *100*, 621−533.
(34) Lee, D.; Choi, M. *J. Aerosol Sci.* **2002**, *33*, 1−16.
(35) Kim, A. S.; Yuan, R. *J. Colloid Interface Sci.* **2005**, *285*, 627−633.

a geometrical configuration of the aggregates covered with the EDL having a thickness t in nanofluid.

Step 1. Primary Particle Covered with Interfacial Layer. As a first step, a primary sphere covered with a layer is treated as an imaginary sphere with radius of $a + t$. The volume fraction ϕ_1 of the core solid sphere in the core−shell structure is given by

$$\phi_1 = \left(\frac{a}{a+t}\right)^3 \tag{6}$$

As pH goes far from the point of zero charge (PZC)[14] of CuO in water, with a decrease in t, the ϕ_1 value increases up to 14.4%. The Bruggeman effective medium theory (EMT), which is applicable to the whole range of concentration of an inclusion,[17] is used to predict the effective thermal conductivity K_{c^1} of the core−shell sphere by

$$\phi_1\left[\frac{K_s - K_{c^1}}{K_s + 2K_{c^1}}\right] + (1-\phi_1)\left[\frac{K_l - K_{c^1}}{K_l + 2K_{c^1}}\right] = 0 \tag{7}$$

where K_s and K_l have the same meanings as in eq 2. An explicit expression of K_{c^1} is obtained by solving eq 7 for K_{c^1} as

$$K_{c^1} = \frac{1}{4}[3\phi_1(K_s - K_l) + (2K_l - K_s) + \sqrt{A}] \tag{8}$$

where the term A is given by $A = [3\phi_1(K_s - K_l) + (2K_l - K_s)]^2 + 8K_sK_l$.

Step 2. An Aggregate Consisting of the Core−Shell Primary Particles. An aggregate with an interfacial layer is modeled as a solid-phase element of another imaginary sphere with radius of $R + t$ (see Figure 3). A volume fraction ϕ_2 of the liquid-layered aggregate in the imaginary sphere is accordingly given by

$$\phi_2 = \frac{(a+t)^3 N_p}{(R+t)^3} \tag{9}$$

The Bruggeman model is again used to yield the thermal conductivity K_{c^2} of the second imaginary sphere containing the aggregate, layer, and liquid. As the liquid-layered aggregate becomes a new solid fraction in the model, K_s and K_{c^1} in eq 7 are replaced by K_{c^1} and K_{c^2}, respectively

$$\phi_2\left[\frac{K_{c^1} - K_{c^2}}{K_{c^1} + 2K_{c^2}}\right] + (1-\phi_2)\left[\frac{K_f - K_{c^2}K_{c^2}}{K_f + 2K_{c^2}}\right] = 0 \tag{10}$$

Step 3. The Whole System where the Second Imaginary Spheres Are Suspended. As number concentration (n) of the imaginary spheres should be identical to that of the original aggregates, it is determined by dividing the original volume fraction (ϕ_{exp}) of particles by mean volume (v_a) of solid-phase aggregates as

$$n = \frac{\phi_{exp}}{v_a} = \frac{3\phi_{exp}}{N_p 4\pi a^3} \tag{11}$$

The product of n and mean volume v_s of the imaginary spheres gives the volume fraction ϕ_3 of the spheres in liquid by

$$\phi_3 = nv_s = n\frac{4\pi}{3}(R+t)^3 \tag{12}$$

Assuming that the aggregates are uniformly distributed in liquid, the MG model[17] is finally used to predict the K_{eff} of the nanofluid as

$$\frac{K_{eff}}{K_f} = \frac{(1-\phi_3)(K_{c^2} + 2K_f) + 3\phi_3 K_{c^2}}{(1-\phi_3)(K_{c^2} + 2K_f) + 3\phi_3 K_f} \tag{13}$$

5. Results

A. A Contribution of Brownian Motion of Fractal Aggregates. Again in Figure 1, as pH departs from the isoelectric point of CuO particles (IEP ≈ 8.5), the ζ potential increases gradually along with an increase of surface potential (ψ_0). Since electrostatic repulsion energy between particles is proportional to ζ^2 through DLVO theory,[14,22] the the colloidal system becomes less stable at this time. In this way, particles in liquid get bigger at an unstable pH condition, as seen in Figure 1. The R_h varies by about 48% at most, depending on the pHs. However, the BM model of Kumar et al.[26] for R_h shows that K_{eff} varies by only 1% or less at the moment.

B. Model Prediction for pH Dependence of K_{eff}. Many ions, that exist in the region of $x > \kappa^{-1}$, can be still associated with the afore-mentioned liquid columns, thereby decreasing the potential in the region. Here, the effective thickness of the interface layer is first approximated to double the κ^{-1} ($C = 2$ in eq 1). The value of C is kept constant throughout the predictions in this study. The systematic parameters for the experiment and physical constants used for the model prediction are listed in Table 1. Figure 4 shows that the increment of the effective thermal conductivity ($K_{eff} - K_f$) increases by a factor of 8 as pH decreases from 8 to 3 and the present model successfully predicts the pH dependence. To gain an insight into the pH dependence, any changes in all parameters at various pHs are monitored in Table 2. While decreasing the pH from 8 to 5.6, surface charge states in terms of ionized site density (Γ_{ion}) and charge density (σ_d) are both increased dramatically, but along with the very little increase in ϕ_1. The thermal conductivity of the EDL (K_l) is therefore enhanced by a factor of 2. This in turn increases the K_{c^1} as well as K_{c^2} by almost a factor of 2, subsequently. At this time, the outer radius of equivalent spheres containing aggregates ($R + t$) decreases by only 24%. Thus, the volume fraction of the equivalent spheres ϕ_3 decreases by 27%. In comparison to the changes in the thermal conductivities K_l, K_{c^1}, and K_{c^2}, decreasing volume fraction ϕ_3 generates a minor adverse effect on the K_{eff}. So, it is clear that the abnormal enhancement of the K_{eff} is primarily due to the large increase in the thermal conductivity of the interfacial layer, which might be interpreted as the enhanced phonon transport as inferred before.

C. Prediction of Effects of Temperature, Volume Fraction, and Primary Particle Size. In this section, the present model is further evaluated by comparing the predictions with other experimental results on the effects of temperature, volume fraction, and primary particle size. As indicated at the end of Introduction, surface charge states and fractal information (D_f and R_h) should all be predetermined to give a correct prediction. But, such complete data sets for typical nanofluids have never been reported before. Since the charge states are the fundamental parameters determining D_f and R_h, if the pH values of the colloidal liquids with the same contents are kept constant, the fractal information is likely not varied much. In this regard, the comparisons are limited to the case of CuO−water nanofluids. The data sets at pH = 7 in the previous section are used again for the predictions in this section.

The temperature effect is first chosen, because it has been considered evidence for the BM mechanism. There are two groups[10,15] who experimentally report the temperature effect for CuO−water nanofluids at two different volume loadings of particles. As equilibrium constants (K_p and K_d) for the surface ionization reaction are very sensitive to the temperature

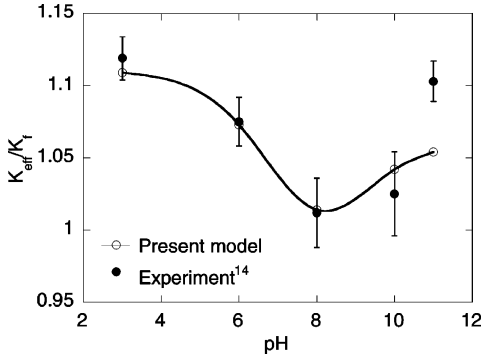

Figure 4. Model prediction of the pH dependence of the effective thermal conductivity of the CuO−water nanofluid; the experiments are made at a volume fraction of 0.003.

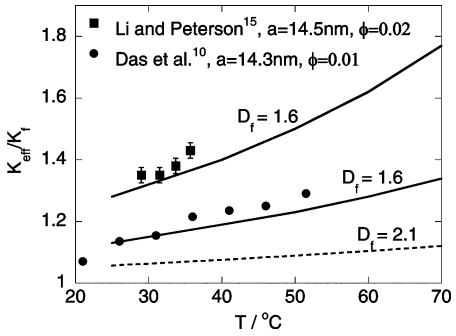

Figure 5. Comparison of the present model with experimental data for CuO−water nanofluid at different temperatures. The solid lines represent the model predictions at the conditions of the two groups, and the dotted line is produced by the model with $D_f = 2.1$ for the condition of Das et al.

T (see eq A3), the surface charge states in terms of Γ_{ion} and σ_d rapidly increases with T, as seen in Table 3, whereas, the thickness κ^{-1} slowly increases with T. Thus, the thermal conductivity of the EDL (K_l in eq 2) has a strong temperature dependence.

As expected, Figure 5 shows that the present interfacial model predicts such a dependence. Also, note that the predictions for two different doses of CuO particles to water are in good agreements with the experiments, which is achieved with no further assumption. To know the effect of particle morphology, i.e., D_f, the prediction for $D_f = 2.1$ is also seen with a dotted line in the figure. At high D_f, in the denser structure of aggregates, the EDL is more often overlapped. This decreases the effective volume fraction ϕ_3 faster than increasing the effective thermal conductivity K_c[2]. Thus, at high D_f, the temperature effect is not as great as at low D_f, which means that open-structured aggregates in suspension is more desirable for enhancing the heat transport. This is consistent with the concept of "clustering" proposed by Keblinski et al.[24]

Second, the effect of volume fraction ϕ_{exp} on the K_{eff} is investigated. The literature data show three distinct differences in the effect, which are highlighted in Figure 6. In Das et al.,[10] the nanofluid with the smallest primary particles has the smallest K_{eff} compared to the others. This seems to contradict the conventional size effect. The K_{eff} of the nanofluid of Eastman et al.[16] linearly increases with particle loadings, while that of Li and Peterson[15] has a flattened ϕ dependence. Why are there such distinct differences even for nanofluids of the same composition? Keblinski et al.[21] recently addressed this, i.e., the lack of agreement between results obtained by different groups, as one of the big obstacles for development. This means that experimentation itself is a challenge. Are these all experimental errors?

Table 1. Parameters Used in the Present Study

experiment	pH = 3−11; $C_{NaCl} = 5 \times 10^{-4}$ mol dm^{-3}; $T = 298$ K; K_f [a] = 0.613 W m^{-1} K^{-1}; $I = 6 \times 10^{-4}$ to 1.5×10^{-3} mol dm^{-3}; $\epsilon_r = 80$ for water; $\phi_{exp} = 0.003$; $d_p = 35$ nm; k_0 [b] = 1.34; D_f [c] = 1.6; K_s [d] = 69 W m^{-1} K^{-1}; for CuO aggregates
model	C in eq 1 = 2.0; a in eq 2 = 0.54
physical constants	$\epsilon_0 = 8.854 \times 10^{-12}$ C V^{-1} m^{-1}; $F = 96\,485$ C mol^{-1}; $R_0 = 8.31$ J mol^{-1} K^{-1}

[a] Mean value of thermal conductivities of base fluids with no particles measured at different pHs. [b] From ref 33. [c] Kept constant throughout the model evaluation unless otherwise noted. [d] From ref 28.

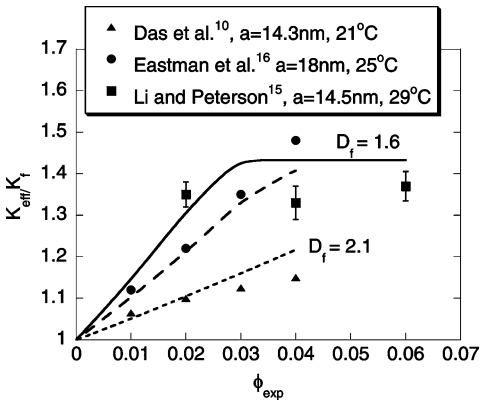

Figure 6. Predictions of the effects of volume fraction for various CuO−water nanofluids at pH = 7. The solid line shows the prediction for the data of Li and Peterson;[15] the dashed line predicts the data of Eastman et al.,[16] and the dotted line predicts the data of Das et al.[10] Note that the prediction for Das et al. is made with $D_f = 2.1$, while $D_f = 1.6$ is used for the others.

The author attempts to answer the question using the present model. As a surprising result, the model predicts reasonably well all of the trends. This implies that the disagreement in experiments reflects differences in some parameters. Li and Petterson's nanofluid contains smaller primary particles at higher temperature than that of Eastman et al. The former nanofluid has the advantage over the latter in effects of size and temperature, which explains the difference in the K_{eff} value at small ϕ_{exp}. The values for D_f and properties of the EDL used for the prediction in Figure 5 are consistently taken for the production of Figure 6. At the same D_f (=1.6) and R_h, if the radius of primary particles a decreases, the number density n of aggregates increases according to eqs 3 and 11, which corresponds to Li and Petterson's case. Also, regarding the fact that the EDL in the case of smaller a is relatively thicker, the effective volume fraction ϕ_3 increases more rapidly than in the nanofluid of Eastman et al. and eventually reaches unity at $\phi_{exp} = 0.03$. That is why K_{eff} of Li and Petterson's nanofluid does not increase further at $\phi_{exp} > 0.03$.

For the data from Das et al. in the figure, the model for $D_f = 1.6$ overestimates their data (not shown here). Rather, $D_f = 2.1$ was found for the best fit, which might be justified by looking at the TEM image of their aggregates.[10] The aggregates have a much more compact structure than our aggregates have (see Figure 1 in ref 14), reflecting higher D_f for their aggregates. One may notice that their data are best fitted with $D_f = 2.1$ at 21 °C and with $D_f = 1.6$ at higher T (see Figure 5). As temperature increases, the surface charge increases along with electrostatic repulsion (see Table 3), which forces primary particles to repel each other, leading to a decrease in D_f. This might be consistent with the sudden increase of the K_{eff} in Figure 5 when T increases from 21 to 25 °C. Does the D_f change in reality? Unfortunately, the author is not in the position to explain what happened exactly

Table 2. Parameters Used for Prediction of the pH Dependence at 25 °C

pH	R_h/nm	κ^{-1}/nm	Γ_{ion}/mol m^{-2}	σ_d/C m^{-2}	ϕ_1	K$_l$/W m^{-1}K^{-1}
3.0	88.4	7.94	5.65×10^{-7}	5.44×10^{-2}	1.44×10^{-1}	19.92
5.6	93.9	13.72	5.29×10^{-8}	5.08×10^{-3}	5.91×10^{-2}	1.73
7.0	111.0	13.75	1.40×10^{-8}	1.29×10^{-3}	5.88×10^{-2}	0.87
8.0	128.2	13.74	4.43×10^{-9}	1.70×10^{-4}	5.89×10^{-2}	0.66
10.0	132.3	12.55	2.56×10^{-8}	-2.44×10^{-3}	6.93×10^{-2}	1.14
11.0	121.7	7.94	8.30×10^{-8}	-7.99×10^{-3}	1.44×10^{-1}	3.04

Table 3. Parameters Used for Prediction of the Temperature Dependence at pH = 7

T/°C	K_p/M^{-1}	K_d/M	k^{-1}/nm	Γ_{ion}/mol m^{-2}	s_d/C m^{-2}	f_1	K_l/W m^{-1} K^{-1}
25	6.00×10^4	2.00×10^{-12}	13.75	1.40×10^{-8}	1.29×10^{-3}	5.88×10^{-2}	0.87
30	7.83×10^4	2.61×10^{-12}	13.86	1.63×10^{-8}	1.49×10^{-3}	5.79×10^{-2}	0.91
40	1.30×10^5	4.34×10^{-12}	14.09	2.16×10^{-8}	1.90×10^{-3}	5.62×10^{-2}	1.01
50	2.09×10^5	6.98×10^{-12}	14.31	2.81×10^{-9}	2.34×10^{-3}	5.46×10^{-2}	1.12
60	3.28×10^5	1.09×10^{-11}	14.53	3.65×10^{-8}	2.80×10^{-3}	5.31×10^{-2}	1.25
70	4.99×10^5	1.66×10^{-11}	14.75	5.55×10^{-8}	2.84×10^{-3}	5.16×10^{-2}	1.42

between 21 and 25 °C, because the necessary data, in particular, the fractal information, is not available.

Finally, the influence of primary particle size is investigated. Regarding the issue of D_f, low D_f (=1.6) is used for the predictions for the nanofluids of Li and Peterson[15] and Eastman et al.,[16] while high D_f (=2.1) is used for those of Das et al.[10] and Lee et al.[11] Since all the literature does not report R_h, the value at pH = 7 in Table 2 is used for the predictions in Figure 7. The figure shows that the model predicts quite well the two distinct trends of experimental data. For the same T and pH, the thermal conductivity and thickness of the interfacial layer is not varied.

As primary particles get smaller in this case, relatively thicker EDL and larger N_p increase ϕ_2 ($\propto 1/a^{Df}$; see eqs 3 and 9) much faster than they decrease ϕ_1 and K_{c^1} (refer to eqs 6 and 7 and Figure 3). This results in a slight increase of K_{c^2} and greater increase in ϕ_3 ($\propto 1/a^{3-Df}$; see eqs 3, 11, 12), which is a primary reason for enhancing the K_{eff}. This explains the rapid increase of the K_{eff} in the region of $a > 10$ nm at $D_f = 1.6$ in Figure 7. As a decreases further from 10 nm, the ϕ_2 reaches unity eventually. Nearly at the same time, the ϕ_3 reaches unity too. In the calculation, once ϕ_2 or ϕ_3 reaches unity, a further increase in each term is not considered. However, K_{c^1} and K_{c^2} keep decreasing slightly due to a decrease of the actual solid fraction in an equivalent sphere with a radius of $R + t$. That is why there exists a maximum in K_{eff} for low D_f. This behavior with respect to the primary particle size was also observed experimentally by Xie et al.[4] for an Al_2O_3−ethylene glycol nanofluid.

For the case of high D_f, aggregates have a denser structure where the EDLs have more chance to be overlapped even for the same a. This means that the ϕ_2 increases to unity faster than for low D_f. However, eq 5 shows that R for $D_f = 2.1$ is smaller than that for $D_f = 1.6$, implying that ϕ_3 increases more slowly than for $D_f = 1.6$. From this reason, the K_{eff} is shown to increase with decreasing a over the whole size range. The predictions with two different fractal dimensions agree reasonably well with two groups of experimental data in Figures 6 and 7. It is likely that the fractal dimensions of the two categorized samples are not the same. Even though the present model resolves successfully the previous anomalies and contradictions in experiments, combining the concepts of fractal and EDL, the author would like to emphasize that the complete data sets such as surface charge states and fractal information should be reported for a better understanding of the abnormal behavior of nanofluids as well as proper evaluation of any theoretical models.

6. Discussion

A. Interpretation of the Conventional Interfacial Layer with Electrical Double Layer. The concept of liquid ordered (or structured) layering has been thought different from the EDL.[37] Molecular ordering at surfaces results in structural and hydration forces. From the other side, EDL force produces electrostatic repulsion. One may have a question about the proximity of the interfacial layer to the EDL. Before discussing it, let me refer to very interesting experimental results[38] where an optical technique such as sum-frequency generation was used to probe liquid molecular orientation at a surface. The results showed that water molecular ordering was greatly pronounced at the SiO_2/water interface as pH increases far from the point of zero charge (PZC) of SiO_2. Also, the paper presented that, at a neutral surface (pH = PZC) of SiO_2, the hydration force induced the single layer ordering by hydrogen bonds, whereas, at a highly charged surface, the spectral intensity corresponding to icelike structure was increased by a factor of 7 from the value at pH = PZC, implying that the electrostatic force induced longer-range orientation of water molecules at the ionized surface. Moreover, it was observed that Na^+ ions existing in the liquid could magnify the influence of electrostatic force on the molecular ordering at an intermediate pH.

These experimental results seem to say that, if the surface is ionized, surface ionized sites are better able to orient polar water molecules and/or counterions (hydrated or not) by hydrogen bonding and/or ionic bonding up to the longer range. Such ion associations should result in a gradual decrease in the potential. This is very similar to the description of Figure 2 and obviously indicates that a new type of ordering can be possible by electrostatic force due to the existence of the EDL. I focused on the electrostatic interaction between particle surface and surrounding water containing ions, rather than between the particles. In this way, the interfacial layer may be interpreted to or approximated with the EDL.

B. The Validity of the Power-Law Relation for Thermal Conductivity of the EDL. The effective thermal conductivity K_{eff} and thermal conductivity of the EDL K_l can display different functional dependence versus $\Gamma_{ion}\sigma_d\kappa$. To determine the validity of the assumption in eq 2, I simulate the behaviors of the K_{c^1}, K_{c^2}, and K_{eff} when independently varying K_l from 0.6 to 20 (highest value at pH = 3). For the purpose of this simulation, other parameters such as ϕ_1, ϕ_2, ϕ_3, κ^{-1}, and R are fixed constant during the simulation with values at pH = 6. As a result, Figure 8 shows that K_{c^1} and K_{c^2} both have nearly linear dependences on K_l, while K_{eff} has a power dependence on K_l. Because K_{eff}

(36) Hiemstra, T.; Van Riemsdijk, W. H.; Bolt, G. H. *J. Colloid Interface Sci.* **1989**, *133*, 91−104 and 105−116.
(37) Israelachvili, J. N. *Intermolecular and Surface Forces*, 2nd ed.; Academic Press: London, 1992.
(38) Du, Q.; Freysz, E.; Shen, Y. R. *Phys. Rev. Lett.* **1994**, *72*, 238−241.

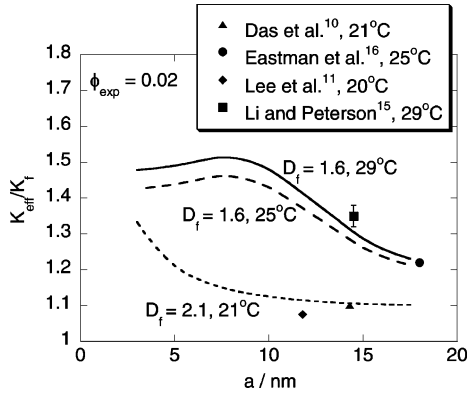

Figure 7. Predictions of the effects of primary particle size for various CuO−water nanofluids at pH = 7 and $\phi = 0.02$. The solid line shows the prediction at $D_f = 1.6$ and $T = 29$ °C, the dashed line predicts the size dependence at $T = 25$ °C, and the dotted line does at $D_f = 2.1$ and $T = 21$ °C.

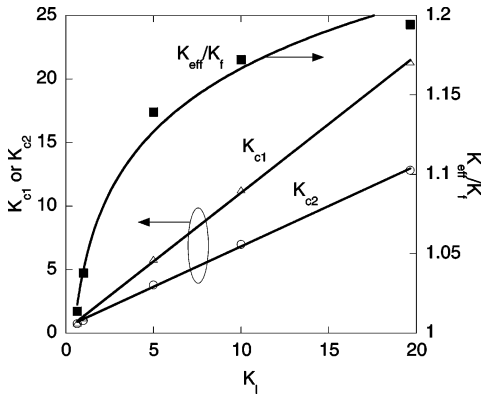

Figure 8. Functional dependences of K_c^1, K_c^2, and K_{eff}/K_f on K_l; solid lines for K_c^1 and K_c^2 represent linear-fitted lines, while the line for K_{eff}/K_f denotes a power-fitted line.

was displayed well with a power function of $\Gamma_{ion}\sigma_d\kappa$ from experiment,[14] it is plausible to assume that K_l has also a power dependence on the $\Gamma_{ion}\sigma_d\kappa$, but the exponents for K_l and K_{eff} would be different.

C. Percolation Behavior of Heat through Aggregate Backbones. As the present model treats an agglomerate enclosed by a liquid sphere (see step 2) as an effective spherical sphere, the percolation should affect the prediction of the effective thermal conductivity K_c^2 of the effective sphere. Therefore, the use of Bruggeman's effective medium theory (EMT) in step 2 has to be justified. Strictly, the EMT corresponds to Bruggeman's symmetric model (BSM), and its use should be restricted for effectively homogeneous and non-fractal media. For fractal and percolating media, the more general effective medium theory (GEM) of McLachlan et al.[39,40] that includes conductivity exponent t' and percolation threshold concentration f_c' should be applied.

According to McLachlan et al.,[39] the percolation thresholds (volume fraction of more conducting inclusions) were not varied much from 0.16 for various lattices. Also, McLachlan[40] suggested that the exponent was related to the threshold as $t' = 3f_c'$ (see p 870 in ref 40). With f_c' and t', K_c^2 at various pHs is estimated by the GEM. The GEM-generated K_c^2 considering the percolation effect was obtained under the assumption of perfect contact between primaries (e.g., sharp prolate ellipsoids), so that K_c^2 would be a upper limit of $K_{c^2,real}$, whereas K_c^2 estimated from BSM in Step 2 would be a lower limit because the symmetric model does not consider the percolation effect.

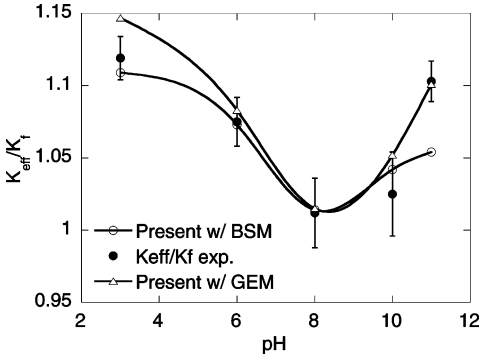

Figure 9. The effect of heat percolation on the K_{eff}.

By applying the $K_{c^2,GEM}$ to the M−G model (eq 13), one may estimate the upper limit of the K_{eff}. Accordingly, the $K_{c^2,BSM}$ presented in Figure 4 corresponds to lower limit. Figure 9 shows a very promising result that the experimental data are between the upper and lower limits. Note that the two limits get close each other in the region of $6 < pH < 10$. A lower surface charge when pH close to PZC leads to a reduction in the contribution of the charge-induced interfacial layer (K_c^1 closer to K_f), so that the percolation effect becomes insignificant.

7. Conclusions

In this study, the author employs the theory of the electrical double layer to investigate the unknown nature of the conventional interfacial layer. On the basis of this conceptual approach, a new fractal model has been developed and evaluated for various systematic parameters. The model was found to predict successfully experimental results for the parameters, i.e., pH, temperature, volume fraction, and primary particle size. Most of the presented data have not been understood by any preexisting models. The chemistry-based nature of the interfacial layer that is introduced in this study seems to play a key role in the control of the thermal conductivity of nanofluids.

Acknowledgment. The author gratefully acknowledges that this work was supported by Korea Research Foundation Grant funded by Korean Government (MOEHRD) (project no. R08-2003-000-10858-0).

Appendix

In our previous work,[14] a theoretical approach, the so-called surface complexation model, to give the surface charge states was introduced in detail. To help understand the nature of the surface charging, a simplified model is presented here. The surface charging arisen when a particle is suspended in a polar liquid is described by[14]

$$\mathrm{MOH} + \mathrm{H}^+ \xrightarrow[K_p]{} \mathrm{MOH_2}^+ \quad K_p = \exp\left(\frac{F\psi_0}{RT}\right)\frac{\Gamma(\mathrm{MOH_2}^+)}{a(\mathrm{H}^+)\Gamma(\mathrm{MOH})}$$

$$\mathrm{MOH} \xrightarrow[K_d]{} \mathrm{MO}^- + \mathrm{H}^+ \quad K_d = \exp\left(-\frac{F\psi_0}{RT}\right)\times \frac{\Gamma(\mathrm{MO}^-)a(\mathrm{H}^+)}{\Gamma(\mathrm{MOH})} \quad \text{(A1)}$$

where M is a metal cation, i.e., Cu(II) in this case, K_p and K_d are equilibrium constants for protonation and deprotonation, respectively, a is activity in the bulk of the solution, and ψ_0 is the surface potential. The equilibrium constants are not inde-

(39) McLachlan, D. S.; Blaszkiewicz, M.; Newnham, R. E. *J. Am. Ceram. Soc.* **1990**, *73*, 2187−2203.
(40) McLachlan, D. S. *J. Phys. C: Solid State Phys.* **1987**, *20*, 865−877.

pendent of each other, but rather interrelated with the point of zero charge (PZC) of particles in water

$$\mathrm{PZC} = \frac{1}{2}\log\left(\frac{K_p}{K_d}\right) \tag{A2}$$

The temperature dependence of the constant K_d is expressed by the van't Hoff equation, and Hiemstra et al.[35] suggested

$$\ln\left[\frac{K_{d,T}}{K_{d,T_0}}\right] = -\frac{\Delta H_0}{R}\left[\frac{1}{T} - \frac{1}{T_0}\right] \tag{A3}$$

The ΔH_0 of metal oxide ranges from 15 to 90 kJ/mol,[35] and 40 kJ/mol was taken for the estimation of the K_d in this study. In this way, when T increases from 25 to 70 °C, each of the K_p and K_d values increases by 1 order of magnitude, as seen in Table 3. At this moment, the charged cites, regardless of their polarities, can be associated further with counterions in the EDL as seen in Figure 2. In the previous work,[14] the surface complexation by the counterions was considered. But at the low concentration of electrolyte, the association effect is quite negligible[22] and therefore neglected in this study. A more simplified model to estimate the surface potential is thus readily derived as follows. The difference between the previous and present models is displayed in Figure 2.

Rearranging the terms in eq A1, the charged site densities ($\Gamma(MOH_2^+)$ and $\Gamma(MO^-)$) are expressed as a function of uncharged site density $\Gamma(MOH)$. The total sum of charged and uncharged site densities is equal to the total surface site density Γ_{tot} (ca. 5.9×10^{-6} mol/m^2).[14] Using this, one can easily derive the following equations

$$\Gamma(MOH) = \frac{\Gamma_{tot}}{1 + a_s(H^+)K_p + K_d/a_s(H^+)} \tag{A4}$$

$$\Gamma(MOH_2^+) = \frac{\Gamma_{tot}a_s(H^+)K_p}{1 + a_s(H^+)K_p + K_d/a_s(H^+)} \tag{A5}$$

$$\Gamma(MO^-) = \frac{\Gamma_{tot}K_d/a_s(H^+)}{1 + a_s(H^+)K_p + K_d/a_s(H^+)} \tag{A6}$$

where the activity of H^+ at the surface is given by the Maxwell−Boltzman distribution[22]

$$a_s(H^+) \equiv a(H^+)\exp\left(-\frac{F\psi_0}{RT}\right) \tag{A7}$$

A sum of the charged site densities ($\Gamma(MOH_2^+) + \Gamma(MO^-)$) is referred to as Γ_{ion}. Surface charge density σ_0 is given by the definition

$$\sigma_0 = F[\Gamma(MOH_2^+) - \Gamma(MO^-)] = \frac{\Gamma_{tot}F}{1 + a_s(H^+)K_p + K_d/a_s(H^+)}[a_s(H^+)K_p - K_d/a_s(H^+)] \tag{A8}$$

With known values of K_p and K_d at various temperatures, σ_0 is an only function of $a_s(H^+)$ or a function of ψ_0 and T. The σ_0 (approximated to σ_s by the simplified model in Figure 2) is balanced with the charge in the diffuse layer as

$$\sigma_0 = -\sigma_d = -\frac{4FI}{\kappa}\sinh\left(\frac{F\psi_d}{2RT}\right) \approx \frac{4FI}{\kappa}\sinh\left(\frac{F\psi_0}{2RT}\right) \tag{A9}$$

By equating eq A8 to eq A9, one gets a nonlinear equation for ψ_0 and T. At a certain T, numerical iteration for ψ_0 can easily give ψ_0 as a function of T. Once ψ_0 is given, one can obtain all surface site densities and charge density σ_d as well (using eqs A4−6 and A9, respectively).

LA063094K